

# Comparative Study of the Photophysical Properties of Nonplanar Tetraphenylporphyrin and Octaethylporphyrin Diacids

Vladimir S. Chirvony,<sup>\*,1a</sup> Arie van Hoek,<sup>1b</sup> Victor A. Galievsky,<sup>1a</sup> Igor V. Sazanovich,<sup>1a</sup> Tjeerd J. Schaafsma,<sup>1b</sup> and Dewey Holten<sup>\*,1c</sup>

*Institute of Molecular and Atomic Physics, National Academy of Sciences of Belarus, F. Skaryna Ave. 70, Minsk 220072, Belarus, and Laboratory of Molecular Physics, Department of Biomolecular Sciences, Agricultural University, Dreijenlaan 3, 6703 HA Wageningen, The Netherlands, and Department of Chemistry, Washington University, St. Louis, Missouri 63130*

Received: April 27, 2000; In Final Form: August 18, 2000

The photophysical properties of the lowest excited singlet states,  $S_1(\pi, \pi^*)$ , of two porphyrin diacids have been investigated. The diacids are  $H_4TPP^{2+}$  and  $H_4OEP^{2+}$ , the diprotonated forms of free base tetraphenylporphyrin ( $H_2TPP$ ) and octaethylporphyrin ( $H_2OEP$ ), respectively. Both diacids exhibit perturbed static and dynamic characteristics relative to the parent neutral complexes in solution at room temperature. These properties include enhanced yields of  $S_1 \rightarrow S_0$  radiationless deactivation (internal conversion), which increase from  $\sim 0.1$  for  $H_2TPP$  and  $H_2OEP$  to 0.4 for  $H_4OEP^{2+}$  and 0.6 for  $H_4TPP^{2+}$ . The fluorescence lifetimes of both diacids are strongly temperature dependent, with an activation enthalpy of  $\sim 1400 \text{ cm}^{-1}$  for  $S_1$ -state deactivation. The enhanced nonradiative decays and many other photophysical consequences of diacid formation are attributed primarily to nonplanar macrocycle distortions. Both  $H_4TPP^{2+}$  and  $H_4OEP^{2+}$  have been shown previously by X-ray crystallography to adopt saddle-shaped conformations, and the magnitudes of the perturbed properties for the two diacids in solution correlate with the extent of the deviations from planarity in the crystals. A model is proposed to explain the nonradiative decay behavior of the porphyrin diacids that is relevant to nonplanar porphyrins in general. The model includes the existence of decay funnels on the  $S_1(\pi, \pi^*)$ -state energy surface that are separated from the equilibrium conformation and other minima by activation barriers. It is suggested that these funnels involve configurations at which the potential-energy surfaces of the ground and excited states approach more closely than at the equilibrium excited-state structure(s) from which steady-state fluorescence occurs. Possible contributions to the relevant nuclear coordinates are discussed.

## Introduction

Recent studies have demonstrated that the photophysical properties of nonplanar porphyrins differ significantly from those of their planar analogues.<sup>2,3</sup> The main differences are: (1) shifts to longer wavelengths of the electronic ground-state absorption bands, (2) large spacings between the fluorescence and long-wavelength absorption maxima (i.e., large “Stokes” shifts), (3) reduced structure and increased breadth of the fluorescence emission, and (4) reduced fluorescence yields and shortened lifetimes of the  $S_1(\pi, \pi^*)$  excited states due primarily to enhanced internal conversion to the ground state. The nonplanar distortions (e.g., ruffle, saddle, etc.) of the macrocycle in these systems are generally induced by nonspecific steric interactions involving multiple and/or bulky peripheral substituents (e.g., octaethyltetraphenyl, dodecaphenyl, and tetra-*tert*-butyl porphyrins).<sup>4</sup>

Nonplanar distortions of the porphyrin core also can be induced without such modifications to the periphery of the essentially planar parent compound. These distortions are realized by the addition of two protons (for a total of four) to the tertiary nitrogens of the porphyrin core to form the diacid, also called the dication (Figure 1). Such diprotonation can be achieved in organic solvents by the addition of acid, trifluoroacetic acid being a common reagent. In the diacid adducts, there appears to be close interactions between the diprotonated

porphyrin and the conjugate bases of two acid molecules, such as hydrogen bonding to the central nitrogens.<sup>5,6</sup> For example, the tetraphenylporphyrin diacid formed by reaction of  $H_2TPP$  and  $CF_3COOH$  is best represented as  $[H_4TPP](CF_3COO)_2$ , which will be denoted  $H_4TPP^{2+}$ . Porphyrin diacids typically have nonplanar structures with mainly saddle-type distortions, as revealed by X-ray crystallography, although other structures can be realized depending, for example, on the acid reagent used.<sup>6</sup> The deviations from planarity for some diacids, such as saddle-shaped  $H_4TPP^{2+}$ , approach in magnitude those seen in neutral saddle-shaped dodeca-substituted porphyrins such as free base octaethyltetraphenylporphyrin ( $H_2OETPP$ ) and dodecaphenylporphyrin ( $H_2DPP$ );<sup>4</sup> the diacids of these highly substituted porphyrins exhibit even larger distortions.<sup>7</sup> However, the diacids of  $H_2TPP$  and  $H_2OEP$  lack the additional electronic influence and solvent interactions of the extra peripheral substituents that may contribute to the properties of the highly substituted porphyrins. Thus, the diacids provide an opportunity to study in more pure form the influence of the macrocycle nonplanarity on static and dynamic photophysical properties.

The diacids exhibit a number of perturbed photophysical properties compared to their neutral parent complexes.<sup>8–11</sup> In an early study performed over 20 years ago, a quantum yield of triplet-state formation ( $S_1 \rightarrow T_1$ ) of  $\Phi_T = 0.26$  was found for the tetraphenylporphyrin diacid ( $H_4TPP^{2+}$ ).<sup>8</sup> This value is substantially lower than  $\Phi_T = 0.70–0.85$  for the neutral parent

\* To whom reprint requests should be addressed. E-mail: chirvony@imaph.bas-net.by and holten@wuchem.wustl.edu.

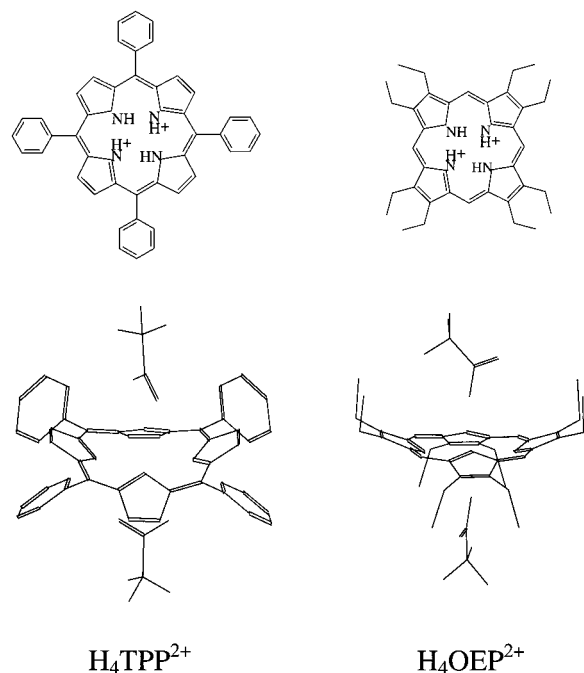


**Figure 1.** Structures of the diacids  $H_4TPP^{2+}$  (left) and  $H_4OEP^{2+}$  (right). For each molecule, an energy-minimized structure obtained from semiempirical calculations (PM3 method implemented in HyperChem (Hypercube, Inc.) software) is shown, including the two  $CF_3COO^-$  species from the acid reagents that are hydrogen-bonded to the central nitrogens and seen in the X-ray structures.<sup>6</sup> The nonplanar distortions in these energy-minimized structures are comparable to those seen in X-ray data.

free-base porphyrin  $H_2TPP$ .<sup>12</sup> The  $S_1 \rightarrow S_0$  fluorescence quantum yield of  $\Phi_F \approx 0.1$  did not differ markedly for  $H_4TPP^{2+}$  and  $H_2TPP$ . These findings indicate that the quantum yield of  $S_1 \rightarrow S_0$  internal conversion ( $\Phi_{IC} = 1 - \Phi_F - \Phi_T$ ) has increased dramatically to  $\Phi_{IC} \approx 0.65$  for  $H_4TPP^{2+}$  from 0.1 to 0.2 for  $H_2TPP$ . However, the reasons for substantially enhanced  $S_1$ -state nonradiative decay in the diacid were not delineated. Recently, two studies have offered different explanations for the unusual excited-state deactivation behavior of  $H_4TPP^{2+}$ .<sup>10,11</sup> In one study, the increased rate of internal conversion in this diacid was ascribed to macrocycle nonplanarity, by analogy with photophysics of highly substituted neutral distorted porphyrins such as  $H_2DPP$ .<sup>10</sup> In the other study, the enhanced nonradiative decay was attributed to quenching of the  $S_1(\pi, \pi^*)$  state via a low-lying electronic state involving charge transfer between the macrocycle and the peripheral phenyl rings, with the charge-transfer process facilitated by the near coplanar disposition of the phenyl groups relative to the neighboring pyrrole rings.<sup>11</sup>

Here we have compared the photophysical properties of the neutral forms and the diacid derivatives of the benchmark free base tetraphenyl and octaethyl porphyrins ( $H_2TPP$  and  $H_2OEP$ , respectively). For all four compounds, fluorescence decay profiles were determined with high accuracy using time-correlated single-photon counting, and other photophysical properties were measured. The available crystallographic structural information for these diacids<sup>6</sup> has enabled us to find a correlation between the photophysical behavior and the ground-state distortions and flexibility of the porphyrin macrocycle in the diacids relative to the neutral complexes. A mechanism involving deactivation funnels on the excited-state surface is proposed to explain the enhanced nonradiative decay properties of the porphyrin diacids, and is applicable to nonplanar porphyrins in general.

## Experimental Section

5,10,15,20-tetraphenylporphyrin ( $H_2TPP$ ) and 2,3,7,8,12,13,17,18-octaethylporphyrin ( $H_2OEP$ ) were synthesized following literature methods.<sup>13</sup> Diacid species  $[H_4TPP](CF_3COO)_2$  and  $[H_4OEP](CF_3COO)_2$  ( $H_4TPP^{2+}$  and  $H_4OEP^{2+}$ , respectively) were prepared by adding trifluoroacetic acid (TFA, 5 vol %) into solutions of the corresponding neutral porphyrins.

Absorption spectra were recorded using a Cary 500 Scan spectrophotometer. Corrected steady-state fluorescence and fluorescence excitation spectra were recorded on an SDL-2 fluorescence spectrometer (LOMO production, Russia) with right-angle detection; spectra were collected out to 1100 nm. For steady-state fluorescence measurements, we used a  $90^\circ$  angle between the excitation and the detection directions.

Time-resolved fluorescence measurements were carried out using time-correlated single-photon counting as described earlier.<sup>14</sup> The pulse duration of excitation pulses was  $\sim 4$  ps full width at half-maximum (fwhm), the maximum pulse energy was  $\sim 100$  pJ, and the excitation wavelength could be tuned over the entire visible and near-UV regions. Samples for the fluorescence kinetics measurements were placed in  $0.5$  cm<sup>3</sup>, 1 cm light-path fused silica cuvettes. The emission was selected via a polarizer set at the magic angle ( $54.7^\circ$ ) with respect to the electric vector of the excitation light. The fluorescence was collected at an angle of  $90^\circ$  with respect to the direction of the exciting light beam. A monochromator was used for wavelength selection of emission. Detection electronics were standard time-correlated single-photon counting modules containing some additional improvements.<sup>14b</sup> The instrument response function was  $\sim 35$  ps fwhm. A reference light-scattering sample was used to obtain an instrument response function as a reference for deconvolution of the fluorescence-lifetime profiles.<sup>14c</sup> Data analysis was performed on a personal computer with homemade software.

Quantum yields of the lowest excited triplet state formation ( $\Phi_T$ ) were determined by two methods. The first was the comparison method<sup>15a</sup> using triplet-state transient absorption techniques<sup>15b</sup> and an  $H_2OEP$  standard<sup>12a</sup> ( $\Phi_T = 0.85$ ). The second method utilized porphyrin-sensitized singlet oxygen generation and a comparison method<sup>15b</sup> using a PdOEP standard<sup>15</sup> ( $\Phi_T = 1.0$ ); it was assumed that the quantum yield of the singlet oxygen generation is equal to the quantum yield of triplet state formation for the compounds under study, which is typically the case for the normal porphyrins.<sup>16,17</sup> The two methods gave similar  $\Phi_T$  values for each of the porphyrin diacids.

All measurements were carried out in toluene solutions containing dissolved oxygen (from air). The effects of air-equilibrated dissolved oxygen on the lifetimes of the parent neutral free base porphyrins  $H_2OEP$  and  $H_2TPP$  are well documented (e.g., shortening the lifetime of  $H_2TPP$  from  $\sim 13$  to  $\sim 10$  ns). The effect on the measured fluorescence lifetimes of the corresponding diacids should be no more than  $\sim 10\%$  given that the lifetimes are only several nanoseconds in duration (as is well documented with neutral Zn porphyrins, which have similar lifetimes). Porphyrin concentrations of 10 to 50  $\mu M$  were used.

## Results

**Static Absorption and Fluorescence Spectra.** A distinguishing feature of the  $H_4TPP^{2+}$  ground-state absorption spectrum is that the Q(0,0) band maximum (651 nm) is red-shifted from its position in neutral  $H_2TPP$  (646 nm) (Figure 2). This is an exception to the more general rule that formation of

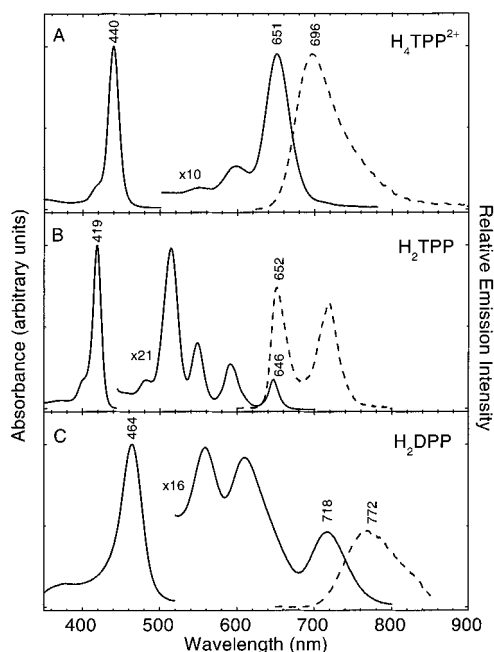


**Figure 2.** Ground-state absorption spectra (solid) and fluorescence spectra (dashed) of  $H_4TPP^{2+}$  (A),  $H_2TPP$  (B) and  $H_2DPP^{3f}$  (C) in toluene at room temperature. The fluorescence maxima and  $Q_x(0,0)$  maxima have been normalized for  $H_4TPP^{2+}$  and  $H_2DPP$  but not for  $H_2TPP$ .

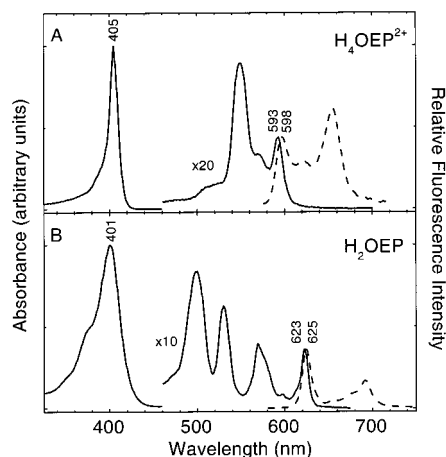


**Figure 3.** Ground-state absorption spectra (solid) and fluorescence spectra (dashed) of  $H_4OEP^{2+}$  (A) and  $H_2OEP$  (B) in toluene at room temperature. The fluorescence and  $Q_x(0,0)$  maxima have been normalized.

a porphyrin diacid from the corresponding neutral free base complex results in a substantial blue shift of the long-wavelength absorption band, as can be seen for  $H_4OEP^{2+}$  in Figure 3.<sup>11</sup> The  $H_4TPP^{2+}$  fluorescence spectrum is also unusual in that it consists of a single broad, structureless feature with a maximum at 696 nm, which is substantially ( $\sim 990\text{ cm}^{-1}$ ) displaced from the absorption maximum (Figure 2A).<sup>9b,11</sup> This emission behavior is again distinct from that of neutral  $H_2TPP$ , which shows well-resolved vibronic structure and a  $Q_x(0,0)$  band that is only modestly ( $\sim 140\text{ cm}^{-1}$ ) displaced from the absorption maximum (Figure 2B). Neither the fluorescence nor the fluorescence-excitation spectrum of  $H_4TPP^{2+}$  changes as the excitation or detection wavelength is varied. As an additional reference compound, the absorption and fluorescence spectra of the sterically crowded nonplanar porphyrin  $H_2DPP$  are shown in Figure 2C. As has been discussed previously, the optical bands of  $H_2DPP$  are red-shifted and broadened compared to

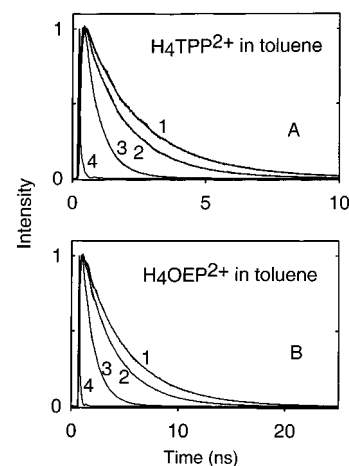


**Figure 4.** Fluorescence decay profiles (at 660 nm) and biexponential fits for the diacids  $H_4TPP^{2+}$  (A) and  $H_4OEP^{2+}$  (B) in toluene at several temperatures (276 K = 1, 300 K = 2, 343 K = 3). Profile 4 is the instrument response function. The resulting lifetime components are given in Table 2.

those of  $H_2TPP$ , with a large ( $\sim 970\text{ cm}^{-1}$ ) spacing between the absorption and fluorescence maxima.<sup>3a,d</sup>

The absorption and emission spectra of  $H_4OEP^{2+}$  are also perturbed from those of its  $H_2OEP$  parent, but in a slightly different manner than for the corresponding TPP complexes. The long-wavelength absorption band of  $H_4OEP^{2+}$  (593 nm) is blue shifted from that for  $H_2OEP$  (623 nm), which is more typical for diacid formation (Figure 3). The emission spectrum of  $H_4OEP^{2+}$  exhibits two resolved features, with a modest ( $\sim 130\text{ cm}^{-1}$ ) spacing between the  $Q(0,0)$  absorption and fluorescence maxima (Figure 3A). The  $H_2OEP$  parent also exhibits well-resolved emission features, but a smaller ( $\sim 50\text{ cm}^{-1}$ ) spacing between the  $Q_x(0,0)$  absorption and fluorescence peaks. Like the  $H_2TPP$  diacid, neither the fluorescence nor the fluorescence-excitation spectrum of  $H_4OEP^{2+}$  changes as the excitation or detection wavelength is varied.

**Fluorescence Lifetimes.** The fluorescence decay profiles for  $H_4TPP^{2+}$  are not monoexponential. Much better fits are obtained with a double-exponential decay model with time constants (and relative amplitudes) of  $\tau_1 = 0.48 \pm 0.08\text{ ns}$  ( $A_1 = 0.24$ ) and  $\tau_2 = 1.73 \pm 0.09\text{ ns}$  ( $A_2 = 0.76$ ) at room temperature (Figure 4A). The major, longer-lived component agrees well with values from single-exponential decays reported previously (Table 1).<sup>9a,11</sup> The relative amplitudes of the two components do not change appreciably across the 660–690 nm region monitored. Both of the lifetime components for  $H_4TPP^{2+}$  lengthen as the temperature is reduced and shorten as the temperature is elevated from room temperature (Figure 4A and Table 2). For example, the lifetime of the major, long-lived component at 660 nm was found to be 2.33 ns at 276 K, 1.73 ns at 300 K and 0.65 ns at 343 K. Preliminary measurements at cryogenic temperatures indicate that the major fluorescence-lifetime component of  $H_4TPP^{2+}$  increases to 5.85 ns at 77 K in toluene/tetrahydrofuran = 1/1 glass (along with a 1.95 ns minor component comprising 20% of the amplitude). An activation enthalpy of 3.7 kcal/mol ( $\sim 1300\text{ cm}^{-1}$ ) was estimated from the 276–343 K data for the  $S_1$ -state decay assuming Arrhenius behavior.

Generally similar fluorescence-decay behavior was found for  $H_4OEP^{2+}$ , with the following differences relative to  $H_4TPP^{2+}$  (Figure 4B and Table 2): (1) The minor, shorter-lived component has a smaller amplitude at all temperatures. (2) The time constants of both fluorescence components (1.5 and 3.3 ns at

**TABLE 1: Photophysical Data for the Porphyrin Diacids and Parent Neutral Complexes<sup>a</sup>**

compd	$\tau_F$ (ns) <sup>b</sup>		$\Phi_F$ <sup>c</sup>		$\Phi_T$ <sup>d</sup>	
	this work	lit.	this work	lit.	this work	lit.
H <sub>4</sub> TPP <sup>2+</sup>	0.48/1.73 (0.24/0.76)	1.8 <sup>e</sup> 1.6 <sup>g</sup>	0.106	0.14 <sup>e</sup> 0.095 <sup>h,i</sup>	0.30	0.26 <sup>f</sup> 0.29 <sup>h,i</sup>
H <sub>4</sub> OEP <sup>2+</sup>	1.51/3.30 (0.20/0.80)	3.5 <sup>e</sup>	0.043	0.052 <sup>e</sup> 0.042 <sup>j</sup>	0.55	
H <sub>2</sub> TPP	5.0/9.8 (0.13/0.87)	10 <sup>i,k</sup>		0.11 <sup>l</sup>		0.70–0.80 <sup>m</sup>
H <sub>2</sub> OEP	10	10 <sup>i,k</sup>		0.16 <sup>k</sup>		0.80–0.85 <sup>m</sup>

<sup>a</sup> Lifetime in solvents containing oxygen from air at room temperature. Toluene was used as solvent in this work and in refs 8, 19c, benzene in refs 9a, 12e, and solvent mixture EPIP (diethyl ether–petroleum ether–2-propanol, 5:5:2) in ref 11. <sup>b</sup> Fluorescence lifetime components and relative amplitudes (in parentheses). <sup>c</sup> Fluorescence quantum yield measured with respect to  $\Phi_F = 0.11$  for H<sub>2</sub>TPP.<sup>31</sup> <sup>d</sup> Quantum yield of triplet state formation. <sup>e</sup> From ref 9a. <sup>f</sup> From ref 8. <sup>g</sup> From ref 11. <sup>h</sup> This value is for the related compound *p*-tetrahydroxyphenylporphyrin in methanol. <sup>i</sup> From ref 12e. <sup>j</sup> From ref 19c. <sup>k</sup> From ref 18. <sup>l</sup> From ref 31. <sup>m</sup> From ref 12.

**TABLE 2: Biexponential Fits of the Fluorescence Decay Profiles of H<sub>4</sub>TPP<sup>2+</sup> and H<sub>4</sub>OEP<sup>2+</sup> in Toluene at Different Temperatures**

compd	temp (K)	decay components (ns)		compd	temp (K)	decay components (ns)	
		1	2			1	2
H <sub>4</sub> TPP <sup>2+</sup>	276	0.53 (0.21)	2.33 (0.79)	H <sub>4</sub> OEP <sup>2+</sup>	276	1.73 (0.15)	4.50 (0.85)
	300	0.48 (0.24)	1.73 (0.76)		300	1.51 (0.20)	3.30 (0.80)
	343	0.26 (0.32)	0.65 (0.68)		343	0.57 (0.14)	1.20 (0.86)

room temperature) are approximately twice as long as those for H<sub>4</sub>TPP<sup>2+</sup> (0.48 and 1.7 ns). Like H<sub>4</sub>TPP<sup>2+</sup>, the fluorescence lifetimes of H<sub>4</sub>OEP<sup>2+</sup> increase as the temperature is reduced, giving an activation enthalpy of 4.0 kcal/mol ( $\sim 1400$  cm<sup>-1</sup>).

As points of reference for the diacids, the fluorescence decays of H<sub>2</sub>TPP and H<sub>2</sub>OEP in toluene at room temperature were also examined. For H<sub>2</sub>TPP, decay profiles were better described with a dual-exponential decay model than a monoexponential function, although the shorter-lived component ( $\sim 5$  ns) represents only  $\sim 10\%$  of the decay. The lifetime of the predominant component ( $9.8 \pm 0.2$  ns) is in good agreement with values reported previously from monoexponential decays in oxygen-containing solvents.<sup>12e,18</sup> The presence of a minor (more short-lived) fluorescence component was found in a number of solvents, using H<sub>2</sub>TPP prepared in a number of laboratories and purchased from several companies. On the other hand, the fluorescence decay profile of H<sub>2</sub>OEP in toluene is well described with a monoexponential function with a time constant of  $10.0 \pm 0.5$  ns.

**Quantum Yields of the S<sub>1</sub>( $\pi,\pi^*$ ) Decay Pathways in the Diacids.** The lowest excited singlet state, S<sub>1</sub>( $\pi,\pi^*$ ), of a porphyrin diacid, like its neutral parent, can decay to the ground state (S<sub>0</sub>) and the lowest excited triplet state (T<sub>1</sub>) by S<sub>1</sub>  $\rightarrow$  S<sub>0</sub> fluorescence emission, S<sub>1</sub>  $\rightarrow$  S<sub>0</sub> nonradiative internal conversion, and S<sub>1</sub>  $\rightarrow$  T<sub>1</sub> nonradiative intersystem crossing. Fluorescence quantum yields in toluene at room temperature are found to be  $\Phi_F = 0.11$  and 0.043, for H<sub>4</sub>TPP<sup>2+</sup> and H<sub>4</sub>OEP<sup>2+</sup>, respectively, in excellent agreement with previous results (Table 1). A triplet quantum yield of  $\Phi_T = 0.30$  was measured for H<sub>4</sub>TPP<sup>2+</sup> in toluene at room temperature, which agrees well with the values of 0.26 and 0.29 determined previously<sup>8,9b</sup> (Table 1). A similar measurement afforded  $\Phi_T = 0.55$  for H<sub>4</sub>OEP<sup>2+</sup>. The triplet

yields for both diacids are lower than  $\Phi_T = 0.70$ – $0.85$  for H<sub>2</sub>-TPP and H<sub>2</sub>OEP,<sup>12</sup> more so for H<sub>4</sub>TPP<sup>2+</sup> than for H<sub>4</sub>OEP<sup>2+</sup>. Internal conversion yields were calculated from the fluorescence and triplet yields using the expression  $\Phi_{IC} = 1 - \Phi_F - \Phi_T$ . The results are  $\Phi_{IC} \sim 0.6$  for H<sub>4</sub>TPP<sup>2+</sup> and  $\Phi_{IC} \sim 0.4$  for H<sub>4</sub>-OEP<sup>2+</sup>. Literature data give  $\Phi_{IC} \sim 0.1$  for both neutral parent complexes H<sub>2</sub>TPP and H<sub>2</sub>OEP (Table 1), which is typical of “normal” porphyrins.<sup>19a,b,f</sup> Thus, S<sub>1</sub>  $\rightarrow$  S<sub>0</sub> nonradiative decay yields are considerably enhanced in the diacids relative to the neutral complexes, more so for H<sub>4</sub>TPP<sup>2+</sup> than for H<sub>4</sub>OEP<sup>2+</sup>. This enhancement of the nonradiative internal conversion pathway is largely responsible for the shortened S<sub>1</sub>( $\pi,\pi^*$ ) lifetimes found for the diacids.

## Discussion

**Origins of the Perturbed Photophysical Properties of the Porphyrin Diacids.** The addition of two more protons to the central nitrogens of the porphyrin macrocycle is expected to have electronic effects on the photophysical properties of the diacids H<sub>4</sub>TPP<sup>2+</sup> and H<sub>4</sub>OEP<sup>2+</sup> relative to H<sub>2</sub>TPP and H<sub>2</sub>OEP. Some of these effects, such as those derived from increased symmetry, are analogous to those that occur upon formation of a corresponding metal derivative (e.g., MgTPP from H<sub>2</sub>TPP). These effects include (1) a collapse of the four main visible-region ground-state absorption bands [Q<sub>Y</sub>(1,0), Q<sub>Y</sub>(0,0), Q<sub>X</sub>(1,0), Q<sub>X</sub>(0,0)] of the neutral complexes to two [Q(1,0) and Q(0,0)], and (2) an associated blue shift of the Q(0,0) band of the diacid (like the metal chelate) from the Q<sub>X</sub>(0,0) band of the neutral free base, namely to a position between the Q<sub>Y</sub>(0,0) and Q<sub>X</sub>(0,0) pair of the parent complex. Such effects are observed for many diacids (like the metal chelates), as has been shown here and previously for H<sub>4</sub>OEP<sup>2+</sup> (Figure 3).<sup>11</sup> However, although H<sub>4</sub>TPP<sup>2+</sup> has the expected two-banded Q-region absorption spectrum, there is a large red shift, not a blue shift, in the long-wavelength Q-band compared to H<sub>2</sub>TPP (Figure 2).

Additionally, relative to the neutral parent complexes, both H<sub>4</sub>TPP<sup>2+</sup> and H<sub>4</sub>OEP<sup>2+</sup> exhibit (1) broadened optical bands, (2) increased spacing between the absorption and emission maxima (i.e., larger “Stokes shifts”), and (3) reduced lifetimes of the predominant (and minor) component of the S<sub>1</sub>( $\pi,\pi$ ) fluorescence decay. All of these effects are larger for H<sub>4</sub>TPP<sup>2+</sup> than for H<sub>4</sub>-OEP<sup>2+</sup>. These findings cannot be explained simply by the electronic effects of diprotonation or increased symmetry. For example, spectral widths and absorption-fluorescence spacings are not significantly altered by metal insertion into the free base compounds, and there is no a priori electronic reason to expect anything different upon diprotonation to form the diacids. Similarly, the insertion of a light metal ion such as Mg(II) that has only a small spin–orbit effect causes only modest changes in the S<sub>1</sub>( $\pi,\pi^*$ ) lifetimes (e.g.,  $\sim 10$  ns for MgTPP and  $\sim 13$  ns for H<sub>2</sub>TPP in deoxygenated solvents). Vibrations involving the central protons do not appear to materially affect S<sub>1</sub>  $\rightarrow$  S<sub>0</sub> internal conversion in free-base porphyrins.<sup>20</sup> These factors indicate that the substantially increased internal conversion rates and the resulting reduced S<sub>1</sub>( $\pi,\pi$ ) lifetimes found in the diacids are not easily understood simply on electronic or vibronic grounds. It has been suggested that the enhanced S<sub>1</sub>  $\rightarrow$  S<sub>0</sub> internal conversion in H<sub>4</sub>TPP<sup>2+</sup> may derive from the participation of a low-energy charge-transfer excited-state involving the macrocycle and the peripheral phenyl rings.<sup>11</sup> It is possible that such a charge-transfer state drops closer to, and mixes more with, the lower-energy S<sub>1</sub>( $\pi,\pi^*$ ) state in the diacid, enhancing nonradiative decay; however, participation of a charge-transfer state cannot additionally explain the perturbed

static optical properties of  $H_4TPP^{2+}$  or the characteristics of  $H_4OEP^{2+}$ , which lacks the peripheral phenyl rings. It is similarly difficult to use purely electronic arguments in general to explain why the photophysical differences between  $H_4TPP^{2+}$  and  $H_2TPP$  are greater than those between  $H_4OEP^{2+}$  and  $H_2OEP$  (Table 1 and Figures 2 and 3).

All of these effects can be understood if diacid formation is accompanied by both purely electronic effects and the (ultimately electronic) consequences of nonplanar distortions. These two sources may complement or counterbalance each other in giving rise to the individual photophysical characteristics of a given diacid, including the magnitude of the differences relative to the neutral complexes; the extent of this balance between these factors may depend, for example, on the magnitude of the deviations of the diacid from planarity. Indeed, conformationally derived effects on the photophysical properties of the diacids are expected for two interrelated reasons:

(1) Both  $H_4TPP^{2+}$  and  $H_4OEP^{2+}$  are known from X-ray crystallography to adopt saddle-shaped structures, in which alternating pyrrole rings are tilted above and below a mean plane containing the *meso* carbons of the macrocycle.<sup>6</sup> The pyrrole-ring  $C_\beta$  carbons are displaced an average  $\sim 1 \text{ \AA}$  with respect to the mean plane for  $H_4TPP^{2+}$  and  $\sim 0.7 \text{ \AA}$  for  $H_4OEP^{2+}$ . The distortions from planarity for  $H_4TPP^{2+}$  approach those exhibited by free base dodecaphenylporphyrin ( $H_2DPP$ ) and octaethyltetraphenylporphyrin ( $H_2OETPP$ ), which have nonplanar saddle-shaped structures as a result of steric interactions involving the multiple peripheral substituents.<sup>4</sup> (Similarly, the diacids of the sterically crowded porphyrins are more nonplanar than their neutral parents.<sup>7</sup>) For  $H_4OEP^{2+}$ , the deviations from planarity are about 30% smaller than for  $H_4TPP^{2+}$ . Thus, the more perturbed photophysical properties of  $H_4TPP^{2+}$  versus  $H_4OEP^{2+}$  correlate with the extent of distortion from planarity seen in the crystallographic data.

(2) The neutral sterically crowded nonplanar porphyrins (e.g.,  $H_2DPP$  and  $H_2OETPP$ ) exhibit dramatic differences in electronic properties compared to the nominally planar analogues (e.g.,  $H_2TPP$  and  $H_2OEP$ ). Indeed, the photophysical characteristics of the diacid  $H_4TPP^{2+}$  have striking similarities to those of  $H_2DPP$ . These comparisons include the red-shifted and broadened absorption and emission bands with large absorption-fluorescence spacings and short  $S_1(\pi, \pi)$  lifetimes (Figure 2 and Table 1). The same is true of  $H_4OEP^{2+}$  relative to neutral nonplanar porphyrins such as  $H_2OETPP$  (with the caveat that the magnitudes of the differences are increased by the four *meso* phenyl rings in the latter complex). The comparisons extend to the tendency of the  $S_1$  lifetimes of both the diacids and many neutral nonplanar porphyrins to lengthen and the static optical properties to change toward those of the nominally planar parent complexes as the temperature is reduced (Tables 1 and 2 and ref 3d). For the  $H_2TPP$  diacid, the electronic effects arising from macrocycle-distortion-induced rotation of the phenyl rings may amplify some of the static-optical perturbations relative to those that occur upon formation of the  $H_2OEP$  diacid. These effects include the magnitude of the red shift in the optical bands of  $H_4TPP^{2+}$  relative to  $H_2TPP$  (due to increased conjugation of the phenyl rings with the macrocycle in the diacid). The absence of the phenyl-ring effects for  $H_4OEP^{2+}$  no doubt contributes to the purely electronic effects of formation of this diacid playing a more significant role relative to the distortion-induced electronic effects than is the case for  $H_4TPP^{2+}$  formation. One result is a net blue shift for  $H_4OEP^{2+}$  versus a red shift for  $H_4TPP^{2+}$  in the long-wavelength optical band compared to the respective parent free base complexes.

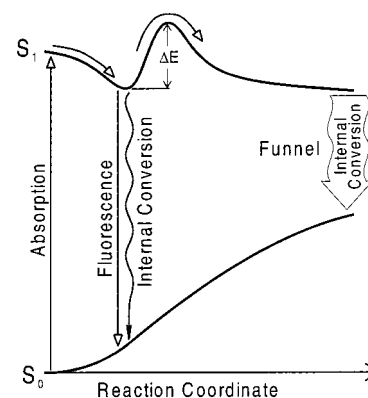


**Figure 5.** Schematic potential-energy surface diagram showing a proposed funnel geometry at which the excited-state nonradiative deactivation is enhanced compared to internal conversion at the equilibrium configuration at which fluorescence is predominantly observed. A small energy barrier must be surmounted to reach the funnel point(s).

The static and time-resolved optical data are most readily understood if the diacids  $H_4TPP^{2+}$  and  $H_4OEP^{2+}$  can (1) change conformation after photoexcitation and (2) access more than one conformation in the ground and/or excited electronic states. These considerations are analogous to the interpretations given previously concerning the sterically crowded nonplanar porphyrins.<sup>3</sup> That there are different equilibrium configurations of the diacid (and solvent) in the  $S_0$  and  $S_1(\pi, \pi^*)$  states, associated with photoinduced structural changes, is indicated by the larger spacings between the absorption and fluorescence maxima found for  $H_4TPP^{2+}$  and  $H_4OEP^{2+}$  relative to  $H_2TPP$  and  $H_2OEP$ . This situation is depicted schematically in Figure 5. This figure also indicates the possibility that conformations other than the one associated with the lowest excited-state minimum may be accessed via barrier crossings. That multiple accessible conformations are energetically close in the ground electronic state (for the diacids and distorted neutral porphyrins) is indicated by the observation that a given nonplanar porphyrin, particularly dodecaphenylporphyrins, can crystallize in more than one form (e.g., saddle, ruffle, or mixtures or variants of these).<sup>4</sup> For example,  $H_2DPP$  crystallizes in both a symmetric saddle conformation and an asymmetric modified saddle conformation.<sup>4b,e,f</sup> Indeed,  $H_2TPP$  itself crystallizes in both a near-planar triclinic structure and  $S_4$ -ruffled tetragonal conformation.<sup>21</sup> It must be noted that the photoinduced conformational changes, and the subsequent excursions about the excited-state equilibrium geometry, do not necessarily involve a complete change in the type of porphyrin nonplanar deformation mode, such as from a saddle to ruffle structure. Rather, they may involve alterations about a given excited-state structure such as asymmetric perturbations of, or addition of ruffle distortions to, a basic saddle shaped structure. Such structural modifications have been seen in various ground-state structures of nonplanar porphyrins.<sup>4</sup> The excited-state configurational changes may also involve the peripheral substituents on the macrocycle and the solvent depending on the system.

A number of observations indicate that the interactions between the nonplanar porphyrin macrocycle and solvent molecules are generally stronger than those involving planar porphyrins, further extending the relevant configurational space.<sup>2g,3e,g,h</sup> These porphyrin-solvent interactions will not necessarily be homogeneous, contributing to the presence of more than one conformer in the ground and excited states in solution, somewhat analogous to the manner in which packing forces can readily induce the existence of multiple ground-

state conformations in the crystals of nonplanar porphyrins. For aryl-substituted porphyrins such as  $H_4TPP^{2+}$ , the conformational degrees of freedom and thus the number of accessible conformations are increased due to the presence of the multiple peripheral aryl rings and their steric and electronic interactions with the solvent. These interactions, which will not be homogeneous, no doubt contribute to the larger spectral widths of  $H_4TPP^{2+}$  relative to  $H_2TPP$  found here and for the related neutral highly substituted nonplanar porphyrins such as  $H_2DPP$  described previously.<sup>3a,d</sup> If the excited-state conformers (involving the macrocycle, peripheral substituents, and solvent) interconvert on a time scale comparable to or shorter than the fluorescence lifetime, then their presence may not be easily resolved in fluorescence excitation measurements (especially if they have similar spectra) but may lead to non-single-exponential excited-state decays, as is observed for the diacids.

The enhanced and temperature-dependent nonradiative decay properties of the diacids (and sterically crowded porphyrins) can be understood in terms of such conformational excursions on the excited-state surface, as is described further below. These conformations would be accessed following motions away from the excited-state configuration(s) formed at the moment of photon absorption. The differences in the magnitudes of the perturbed properties of  $H_4OEP^{2+}$  compared to those of  $H_4TPP^{2+}$  suggest that there are differences in the associated conformational landscapes. The data suggest that the  $H_2OEP$  diacid is (1) less distorted in the ground and excited electronic states, (2) less able to access conformers alternate to the predominate form in either state, and (3) undergoes smaller conformational changes upon photoexcitation. One way to view these differences is that  $H_4OEP^{2+}$  is less "flexible" than  $H_4TPP^{2+}$ . That  $H_4TPP^{2+}$  is not only more distorted but more flexible than  $H_4OEP^{2+}$  has been discussed regarding the X-ray structural data.<sup>6a</sup> A factor that comes into play here, as noted above, is the interactions involving the peripheral phenyl rings of the  $H_2TPP$  diacid, the rotation and tilting of which may be coupled with the nonplanarity of the macrocycle;<sup>7a</sup> these interactions include  $\pi$ -stacking with the aromatic toluene solvent molecules, similar to the situation for  $H_2DPP$  and  $NiDPP$ .<sup>3c,f,h</sup> For  $H_4TPP^{2+}$ , there also may be a connection between the nonplanar conformers giving rise to the dual-exponential fluorescence decays and the (major) near-planar and (minor) ruffled forms that may participate in the similar behavior (with less of a short-lived conformer) for  $H_2TPP$ . Additional factors that contribute, perhaps differently for  $H_4OEP^{2+}$  and  $H_4TPP^{2+}$ , to the conformational landscapes of the diacids (and sterically crowded porphyrins<sup>3</sup>) include the following photoinduced effects: (1) displacement of solvent molecules by out-of-plane motions of the macrocycle, (2) changes in the porphyrin-solvent interactions (polarity, polarizability) if an asymmetric macrocycle structure is accessed, and (3) changes in the interactions of the macrocycle with the conjugate base of the acid reagent (e.g., the  $CF_3COO^-$  groups of  $H_4TPP(CF_3COOH)_2$ ).

**Origin of the Enhanced Nonradiative  $S_1(\pi,\pi^*)$  Decays in the Diacids.** Internal conversion  $S_1 \rightarrow S_0$  is small ( $\Phi_{IC} \sim 0.1$ ) for nominally planar porphyrins such as  $H_2TPP$  and  $H_2OEP$ ;<sup>12</sup> these and other "normal" porphyrins do not contain quenching substituents and/or heavy or open-shell metals that enhance or provide new (e.g., energy- and charge-transfer) excited-state deactivation pathways.<sup>22</sup> Like sterically crowded nonplanar porphyrins,<sup>2,3</sup> both  $H_4TPP^{2+}$  and  $H_4OEP^{2+}$  have much larger internal conversion yields:  $\sim 0.60$  for  $H_4TPP^{2+}$  and  $\sim 0.40$  for  $H_4OEP^{2+}$  at room temperature. We believe that this parameter,  $\Phi_{IC}$ , is in some respects a photophysical integrating parameter

influenced by the degree of the porphyrin macrocycle nonplanarity and conformational flexibility. As noted above, the internal conversion yields measured for  $H_4TPP^{2+}$  and  $H_4OEP^{2+}$  correlate with differences between the two diacids regarding (1) the degree of ground-state nonplanarity seen in the X-ray crystallographic data,<sup>6</sup> and (2) structural excursions in the ground and/or excited electronic states reflected in the static and time-resolved optical data.

What are the means by which macrocycle nonplanarity and flexibility so strongly enhance  $S_1 \rightarrow S_0$  nonradiative decay? The rate of the internal conversion process is governed in part by the vibrational-wave function overlap (Franck–Condon) factor, which is determined by shapes and relationships of the  $S_1$  and  $S_0$  potential-energy surfaces. For typical large aromatic molecules, the ground and excited ( $\pi,\pi^*$ ) electronic states each have a single accessible conformation, each corresponding to the minimum on a relatively harmonic potential energy surface. The  $S_1(\pi,\pi^*)$  and  $S_0$  equilibrium configurations are typically very similar to one another, corresponding to a very small (horizontal) coordinate displacement between the two potential-energy minima, compared to a rather large (typically  $> 1.5$  eV) (vertical) energy gap. Both fluorescence and internal conversion occur out of the single excited-state configuration (potential well). Furthermore, internal conversion follows the familiar energy-gap law for radiationless decay<sup>23</sup> in which the rate decreases exponentially with increasing  $S_1-S_0$  energy gap. Nominally planar porphyrins such as  $H_2TPP$  and  $H_2OEP$  are typical examples: the molecules have large  $S_1-S_0$  energy gaps (1.9–2.1 eV), reflected in the  $Q_X(0,0)$  band positions, and minimal differences in equilibrium structure, reflected in the small (50–150  $cm^{-1}$ ) shifts between the relatively sharp  $Q_X(0,0)$  absorption and emission maxima. In comparison, the diacids and sterically crowded nonplanar porphyrins have significantly larger differences between the equilibrium ground- and excited-state configurations (associated with photoinduced conformational changes), as is indicated by larger absorption-fluorescence spacings. Additionally, for many of these complexes, such as  $H_4TPP^{2+}$  and  $H_2DPP$ , the  $S_1-S_0$  energy gaps are smaller than for the parent  $H_2TPP$ , as is indicated by the red-shifted  $Q(0,0)$  bands. These two effects (larger coordinate displacements and reduced energy gaps) complement each other in enhancing  $S_1 \rightarrow S_0$  internal conversion in the nonplanar complexes.

Although these simple Franck–Condon arguments provide a general means of rationalizing the enhanced  $S_1 \rightarrow S_0$  enhanced nonradiative decay in the diacids and sterically crowded porphyrins, the situation is clearly more complex. Additional factors regarding the mechanisms of internal conversion and the conformational landscapes of the nonplanar porphyrins must be considered. Three examples help to make this point:

(1) The absorption-fluorescence shifts indicate that there is a smaller difference in the  $S_1$  and  $S_0$  equilibrium configurations between  $H_4OEP^{2+}$  and  $H_2OEP$  than there is between  $H_4TPP^{2+}$  and  $H_2TPP$ . This finding is consistent with the lower internal conversion yield of  $H_4OEP^{2+}$  ( $\Phi_{IC} \sim 0.4$ ) versus  $H_4TPP^{2+}$  ( $\sim 0.6$ ), with both being larger than the yield for  $H_2TPP$  ( $\sim 0.1$ ). However, the  $S_1-S_0$  gap for  $H_4OEP^{2+}$  is actually larger than that for the parent  $H_2OEP$ , which would tend to have the opposite effect, namely to diminish nonradiative decay. Although the apparently smaller configurational change could outweigh the larger energy gap for the  $H_2OEP$  diacid relative to its parent  $H_2OEP$ , it is not straightforward to use the simple considerations to quantitatively assess the results on these two complexes in comparison with each other and the  $H_2TPP$  analogues.

(2) The room-temperature absorption-fluorescence spacings for saddle-shaped H<sub>2</sub>DPP (970 cm<sup>-1</sup>) and H<sub>4</sub>TPP<sup>2+</sup> (990 cm<sup>-1</sup>) are larger than those for ruffled H<sub>2</sub>T(*t*-Bu)P (free base *tert*-butylporphyrin) (400 cm<sup>-1</sup>) and H<sub>2</sub>TPP (140 cm<sup>-1</sup>).<sup>3a,d</sup> Similarly, the S<sub>1</sub>–S<sub>0</sub> energy gaps follow the same trend: H<sub>2</sub>DPP > H<sub>4</sub>TPP<sup>2+</sup> > H<sub>2</sub>T(*t*-BuP) > H<sub>2</sub>TPP. However, internal conversion is much more facile for H<sub>2</sub>T(*t*-BuP) (Φ<sub>IC</sub> > 0.8) than for the other complexes, causing the S<sub>1</sub>(π,π\*) lifetime to shorten dramatically to ~50 ps at room temperature.<sup>3b,d</sup> These findings are contrary to the prediction of the simple Franck–Condon arguments: the larger energy gap and apparently smaller photoinduced coordinate displacement both should result in a slower internal conversion rate for H<sub>2</sub>T(*t*-BuP), contrary to observations.

(3) The S<sub>1</sub>(π,π\*) lifetimes and the underlying internal conversion rates of the diacids, like many sterically crowded porphyrins,<sup>3d</sup> increase toward (but remain much different than) those of the planar analogues as the temperature is reduced. [Note that these effects cannot be explained simply by a reversal toward planar ground-state structures at low temperature: for the sterically crowded nonplanar porphyrins, the red-shifted ground-state absorption spectra and many other perturbations are as large, if not larger, at cryogenic temperatures.] These findings are not easily reconciled with standard descriptions of the potential-energy surfaces and nonradiative decay rates that are applicable to planar complexes such as H<sub>2</sub>TPP and H<sub>2</sub>OEP.

These observations and many others for the diacids, and for nonplanar porphyrins in general, are more easily reconciled using the idea, expressed above, that these photoexcited molecules can access multiple configurations on the excited-state surface (conformational flexibility). Again, these configurations may involve distortions about a given nonplanar structure and not necessarily a whole-scale change in the type of macrocycle distortion mode, and may include motions of the peripheral substituents and the solvent. Some of these configurations would contribute to changes in the optical properties of the diacid or neutral nonplanar porphyrin, some to the nonradiative decay properties, and some to both. The key new idea is that the fluorescence and nonradiative decay may not principally occur from the same, single conformation, but from different energetically accessible conformations. Although the fluorescence, and some of the nonradiative deactivation, would occur mainly from the equilibrium configuration (which may consist of a number of close-lying populated configurations of the porphyrin and solvent), there are other accessible excited-state configurations at which internal conversion is greatly enhanced (the “funnel” configuration in Figure 5). Nonradiative decay would be enhanced at these “quenching” configurations because the ground and excited states are even closer energetically due, for example, to added destabilization on the ground-state surface at those points. In the Born–Oppenheimer framework (which likely remains a good approximation at the funnel points if the S<sub>0</sub> and S<sub>1</sub> surfaces are not too close) the rates would again depend on the relevant vibrational-wave function overlaps. The nonradiative decay rates may be additionally enhanced relative to the planar porphyrins at all the accessible conformations due to a strong interplay between the electronic and nuclear degrees of freedom involving the macrocycle, peripheral groups and solvent in the diacids and nonplanar porphyrins. The Born–Oppenheimer breakdown (inseparability of the electronic and nuclear motions) would be particularly acute, giving essentially instantaneous radiationless decay, if S<sub>0</sub> and S<sub>1</sub> become very close or actually touch, and such points are known in the literature as conical intersections (see below).

To access multiple excited-state configurations following photon absorption, barriers must be crossed involving low-energy out-of-plane motions of the porphyrin and motions of the solvent and, if applicable, rotation/tilting of the peripheral phenyl rings on the macrocycle. These barriers seem to have a height of ~1400 cm<sup>-1</sup> for the nonplanar diacids studied here. Similarly, barriers also may need to be crossed in passing from the excited-state configuration formed at the instant of photon absorption to the conformation(s) from which fluorescence predominates.<sup>3f</sup> These barriers contribute to the temperature-dependent photophysics observed here for the diacids, and the temperature and solvent-viscosity-dependent dynamics reported elsewhere for a number of neutral nonplanar porphyrins.<sup>3d,e,h</sup>

Fluorescence may be minimal at the “quenching” excited-state configurations for at least two reasons: (1) The vibrational-overlap factors for the radiative process, which involve the Franck–Condon-active in-plane vibrations (different than the modes participating in nonradiative decay), may be poorer than those at the lowest-energy excited-state configuration. This effect would further decrease the emission amplitude (and increase the spectral bandwidths) compared to the situation at the lowest-energy S<sub>1</sub> configuration, where the emission characteristics are already greatly perturbed from those of the nominally planar complexes. (2) The internal conversion rates at these “quenching” configurations may be sufficiently large so as to overwhelm the radiative probabilities.

The configurations that efficiently return the excited molecule to the ground electronic state have been termed “funnels” in the photochemical literature.<sup>24</sup> The considerations given above suggest that such funnels exist for nonplanar porphyrins, including nonplanar porphyrin diacids. Such a funnel point is indicated schematically in Figure 5. A given nonplanar porphyrin may have a number of such funnel points, that differ in their relationship and thus accessibility (coordinate shift and intervening barrier height) from the predominant excited-state form (lowest-energy excited-state minimum), as well as in their relationship (surface curvature and energy gap) with the ground-state surface; these collective differences will dictate the contributions of the various funnel points to overall S<sub>1</sub> → S<sub>0</sub> internal conversion.

Two main types of funnels have been discussed in the literature: those in which the two electronic surfaces touch (so-called conical intersections) and those in which touching is avoided.<sup>24</sup> The latter situation is depicted in Figure 5, and most likely represents the situation for diacids such as saddle-shaped H<sub>4</sub>TPP<sup>2+</sup> and many sterically crowded porphyrins such as saddle-shaped H<sub>2</sub>DPP. Perhaps in the highly ruffled porphyrins such as H<sub>2</sub>T(*t*-Bu)P or ZnT(*t*-Bu)P, where S<sub>1</sub> lifetimes of 5–50 ps are observed,<sup>3b,d</sup> the situation of a conical intersection of the ground- and excited-state surfaces is more closely approached. Detailed calculations will be required to map out the potential-energy surfaces for these systems and help elucidate the differences in the conformational landscapes for the various types of nonplanar diacids and sterically crowded porphyrins.

The existence of conical intersections in various molecules has been proposed recently on the basis of high-level calculations<sup>25</sup> and used to rationalize experimental results<sup>26</sup> on polyenes and on stilbene isomerization. In the case of *cis*–*trans* ethylene isomerization, *ab initio* calculations suggest that accessing a conical intersection requires pyramidalization of one of the methylene carbons.<sup>27</sup> Although the conformational excursions involving out-of-plane motions in the porphyrin systems are not expected to be as extensive as those occurring in these smaller noncyclic polyene systems, common aspects may exist. A

possible connection is that modification of the hybridization state of the macrocycle carbon atoms in the nonplanar porphyrins may be involved in the nuclear coordinate displacements (the reaction coordinate in Figure 5) leading to funnel configurations. A tendency toward nitrogen-atom pyramidalization in the ground electronic state has been observed for the porphyrin diacids<sup>6d</sup> and monocations<sup>28</sup> and N-trimethylated tetraphenylporphyrin,<sup>29</sup> implying that the hybridization state of the central nitrogens is indeed influenced by porphyrin-macrocycle nonplanarity. In this regard, it is interesting that a zinc isoporphyrin, a tautomer bearing a saturated sp<sup>3</sup> meso-carbon, has photophysical properties very similar to those of the nonplanar porphyrins.<sup>3d,30</sup> Note that a modification of the hybridization state of one or more macrocycle atoms is only one possible reaction coordinate leading to the funnel points depicted in Figure 5. Whatever the specific origin, our model suggests that the conformational flexibility of the photoexcited nonplanar porphyrins (involving the macrocycle, peripheral substituents and solvent) allows access, via barrier crossings, to nonplanar configurations that have reduced energy gaps between the ground and excited states (due principally to a large HOMO destabilization<sup>2a,4a</sup>), with dramatic consequent effects on the static and dynamic photophysical behavior. High-level calculations will be required to examine this issue in more detail and elucidate the underlying physical origins driving the conformational dynamics indicated by a wide variety of observations on the nonplanar porphyrins, including our results on the porphyrin diacids.

## Conclusions

The photophysical properties of nonplanar porphyrin diacids H<sub>4</sub>TPP<sup>2+</sup> and H<sub>4</sub>OEP<sup>2+</sup> resemble in many ways those of neutral sterically crowded nonplanar porphyrins. One of these properties is enhanced S<sub>1</sub> → S<sub>0</sub> internal conversion relative to the nominally planar analogues. For the two diacids, the magnitude of the perturbations to the photophysical properties correlates with the degree of nonplanarity in the ground state. For the diacids, and nonplanar porphyrins in general, the ground-state distortions may be accompanied by conformational flexibility: the molecules are able to access additional nonplanar conformations in the ground and/or excited electronic states, and they are prone to photoinduced conformational changes. A new model that incorporates and extends previous interpretations is proposed to more fully understand the unusual behavior of the nonplanar (diacid and sterically crowded) porphyrins. For these molecules, fluorescence predominantly occurs from the lowest-energy excited-state configuration (just as for planar porphyrins) or a group of accessible forms, but the equilibrium configuration(s) is different from that for the S<sub>0</sub> state. Furthermore, although S<sub>1</sub> → S<sub>0</sub> nonradiative internal conversion occurs to some extent from this same configuration, it takes place mainly from other configurations that have smaller energy gaps from the ground state (funnel points). The conformational excursions leading to these quenching configurations require barrier crossings, giving rise to temperature- (and solvent-) dependent properties. Differences in the extent of out-of-plane distortions and conformational flexibility among different nonplanar porphyrins together give rise to the varied and, in some cases, novel photophysical properties exhibited by these molecules.

**Acknowledgment.** This material is based upon work supported by the U.S. Civilian Research and Development Foundation under Award No BC1-105 (to V.S.C., V.A.G. and D.H.) and a grant from the National Institutes of Health (GM34685 to D.H.) Authors are also grateful to the State Committee for

Science and Technology of the Republic of Belarus and INTAS for the financial support (Grant INTAS-Belarus No 97-0428) and to Dr. N. N. Kruk and Dr. S. M. Bachilo for the measurements of the triplet state quantum yields.

## References and Notes

- (1) (a) National Academy of Sciences of Belarus. (b) Agricultural University of Wageningen. (c) Washington University.
- (2) (a) Barkigia, K. M.; Chantranupong, L.; Smith, K. M.; Fajer, J. *J. Am. Chem. Soc.* **1988**, *110*, 7566. (b) Jentzen, W.; Simpson, M. C.; Hobbs, J. D.; Song, X.; Ema, T.; Nelson, N. Y.; Medforth, C. J.; Smith, K. M.; Veyrat, M.; Mazzanti, M.; Ramasseul, R.; Marchon, J.-C.; Takeuchi, T.; Goddard, W. A.; III.; Shelnut, J. A. *J. Am. Chem. Soc.* **1995**, *117*, 11085. (c) Takeda, J.; Ohya, T.; Sato, M. *Chem. Phys. Lett.* **1991**, *183*, 384. (d) Charlesworth, P.; Truscott, T. G.; Kessel, D.; Medforth, C. J.; Smith, K. M. *J. Chem. Soc., Faraday Trans.* **1994**, *90*, 1073. (e) Ravikanth, M.; Chandashekar, T. K. *Struct. Bond.* **1995**. (f) Barkigia, K. M.; Berber, M. D.; Fajer, J.; Medforth, C. J.; Renner, M. W.; Smith, K. M. *J. Am. Chem. Soc.* **1990**, *112*, 8851. (g) Takeda, J.; Sato, M. *Chem. Lett.* **1991**, 971.
- (3) (a) Gentemann, S.; Medforth, C. J.; Forsyth, T. P.; Nurco, D. J.; Smith, K. M.; Fajer, J.; Holten, D. *J. Am. Chem. Soc.* **1994**, *116*, 7363. (b) Gentemann, S.; Medforth, C. J.; Ema, T.; Nelson, N. Y.; Smith, K. M.; Fajer, J.; Holten, D. *Chem. Phys. Lett.* **1995**, *245*, 441. (c) Drain, D. M.; Kirmaier, C.; Medforth, C. J.; Nurco, D. J.; Smith, K. M.; Holten, D. *J. Phys. Chem.* **1996**, *100*, 11984. (d) Gentemann, S.; Nelson, N. Y.; Jaquinod, L.; Nurco, D. J.; Leung, S. H.; Medforth, C. J.; Smith, K. M.; Fajer, J.; Holten, D. *J. Phys. Chem. B* **1997**, *101*, 1247. (e) Drain, C. M.; Gentemann, S.; Roberts, J. A.; Nelson, N. Y.; Medforth, C. J.; Jia, S.; Simpson, M. C.; Smith, K. M.; Fajer, J.; Shelnut, J. A.; Holten, D. *J. Am. Chem. Soc.* **1998**, *120*, 3781. (f) Retsek, J. L.; Gentemann, S.; Medforth, C. J.; Smith, K. M.; Chirvony, V. S.; Fajer, J.; Holten, D. *J. Phys. Chem.* **2000**, *104*, 6690. (g) Chirvony, V. S.; Sazanovich, I. V.; Galievsky, V. A.; van Hoek, A.; Schaafsma, T. J.; Malinovskii, V. L.; Holten, D. Manuscript in preparation. (h) Retsek, J. L.; Nurco, D. J.; Medforth, C. J.; Smith, K. M.; Sazanovich, I. V.; Chirvony, V. S.; Holten, D. Manuscript in preparation.
- (4) (a) Barkigia, K. M.; Berber, M. D.; Fajer, J.; Medforth, C. J.; Renner, M. W.; Smith, K. M. *J. Am. Chem. Soc.* **1990**, *112*, 8851. (b) Medforth, C. J.; Senge, M. O.; Smith, K. M.; Sparks, L. D.; Shelnut, J. A. *J. Am. Chem. Soc.* **1992**, *114*, 9859. (c) Barkigia, K. M.; Renner, M. W.; Ferunlid, L. R.; Medforth, C. J.; Smith, K. M. *J. Am. Chem. Soc.* **1993**, *115*, 3627. (d) Nurco, D. J.; Medforth, C. J.; Forsyth, T. P.; Olmstead, M. M.; Smith, K. M. *J. Am. Chem. Soc.* **1996**, *118*, 10918. (e) Barkigia, K. M.; Nurco, D. J.; Renner, M. W.; Melamed, D.; Smith, K. M.; Fajer, J. *J. Phys. Chem. B* **1998**, *102*, 322. (f) Senge, M. O. *Z. Naturforsch.* **1999**, *54b*, 821.
- (5) (a) Gradyushko, A. T.; Knyukshto, V. N.; Solovyov, K. N.; Tsvirko, M. P. *Zh. Prikl. Spekt.* **1975**, *23*, 444. (b) Berezin, B. D. *Zh. Obshch. Khim.* **1973**, *43*, 2738.
- (6) (a) Cheng, B.; O. Q. Munro, H. M. Marques, W. R. Scheidt *J. Am. Chem. Soc.* **1997**, *119*, 10732. (b) Reference 20 in ref 6a. (c) Stone, A.; Fleischer, E. B. *J. Am. Chem. Soc.* **1968**, *90*, 2735. (d) Cetinkaya, E.; Johnson, A. W.; Lappert, M. F.; McLaughlin, G. M.; Muir, K. W. *J. Chem. Soc., Dalton Trans.* **1974**, 1236.
- (7) (a) Senge, M. O.; Forsyth, T. P.; Nguyen, L. T.; Smith, K. M. *Angew. Chem., Int. Ed. Engl.* **1994**, *33*, 2485. (b) Barkigia, K. M.; Fajer, J.; Berber, M. D.; Smith, K. M. *Acta Crystallogr.* **1995**, *C51*, 511.
- (8) Chirvony, V. S.; Sagun, E. I.; Dzharagorov, B. M. *Zh. Prikl. Spektrosk.* **1977**, *27*, 167.
- (9) (a) Ohno, O.; Kaizu, Y.; Kobayashi, H. *J. Phys. Chem.* **1985**, *82*, 1779. (b) Akins, D. L.; Zhu, H.-R.; Guo, C. *J. Phys. Chem.* **1996**, *100*, 5420.
- (10) Chirvony, V. S. In Abstracts, Terenin Memorial International Symposium on Photochemistry and Photophysics of Molecules and Ions, St. Petersburg, 1996; pp 163–164.
- (11) Knyukshto, V. N.; Solovyov, K. N.; Egorova, G. D. *Biospectroscopy* **1998**, *4*, 121.
- (12) (a) Gradyushko, A. T.; Sevchenko, A. N.; Solovyov, K. N.; Tsvirko, M. P. *Photochem. Photobiol.* **1970**, *11*, 387. (b) Dzharagorov, B. M. *Izv. AN SSSR, Ser. Fiz.* **1972**, *36*, 1093. (c) Kajii, Y.; Obi, K.; Tanaka, I.; Tobita, S. *Chem. Phys. Lett.* **1984**, *111*, 347. (d) Kikuchi, K.; Kurabayashi, Y.; Kokubun, H.; Kaizu, Y.; Kobayashi, H. *J. Photochem. Photobiol. A: Chem.* **1988**, *45*, 261. (e) Bonnett, R. D.; McGarvey, D. J.; Harriman, A.; Land, E. J.; Truscott, T. G.; Winfield, U.-J. *Photochem. Photobiol.* **1988**, *48*, 271.
- (13) (a) Little, R. G.; Anton, J. A.; Loach, P. A.; Ibers, J. A. *J. Heterocycl. Chem.* **1975**, *12*, 343. (b) Whitlock, H. W.; Hanauer, R. J. *Org. Chem.* **1968**, *33*, 2169.
- (14) (a) Bruggeman, Y. E.; Boogert, A.; van Hoek, A.; Jones, P. T.; Winter, G.; Schots,.; Hillhorst, R. *FEBS Lett.* **1996**, *388*, 242. (b) van Hoek, A.; Visser, A. J. W. G. *Anal. Instrum.* **1985**, *14*, 359. (c) Vos, K.; van Hoek, A.; Visser, A. J. W. G. *Eur. J. Biochem.* **1987**, *165*, 55.



- (15) (a) Kruk, N. N.; Dzhagarov, B. M.; Galievsky, V. A.; Chirvony, V. S.; Turpin, P.-Y.; *J. Photochem. Photobiol. B: Biol.* **1998**, *42*, 181. (b) Bowers, P. I.; Porter, G. *Proc. R. Soc.* **1967**, *296A*, 435.
- (16) Solovyov, K. N.; Tsvirko, M. P.; Sapunov, V. V. *Zh. Prikl. Spekt.* **1978**, *18*, 733.
- (17) Dzhagarov, B. M.; Gurinovich, G. P.; Novichenkov, V. E.; Salokhiddinov, K. I.; Shulga, A. M.; Ganzha, V. A. *Khim. Fiz.* **1987**, *6*, 1069.
- (18) Gradyushko, A. T.; Tsvirko, M. P. *Opt. Spektrosk.* **1971**, *31*, 291.
- (19) (a) Dzhagarov, B. M. *Opt. Spektrosk.* **1970**, *28*, 66. (b) Solovyov, K. N.; Knyukshto, A. V.; Tsvirko, M. P.; Gradyushko, A. T. *Opt. Spekt.* **1976**, *6*, 964. (c) Fonda, H. N.; Gilbert, J. V.; Cormier, R. A.; Sprague, J. R.; Kamioka, K.; Connolly, J. S. *J. Phys. Chem.* **1993**, *97*, 7024. (d) Knyukshto, V. N.; Shul'ga, A. M.; Sagun, E. I.; Zenkevich, E. I. *Zh. Prikl. Spekt.* **1998**, *65*, 900.
- (20) Sagun, E. I. *Khim. Fiz.* **1990**, *9*, 764.
- (21) (a) Silvers, S. J.; Tulinsky, A. *J. Am. Chem. Soc.* **1967**, *89*, 3331. (b) Silvers, S. J.; Tulinsky, A. *J. Am. Chem. Soc.* **1964**, *86*, 927. (c) Hamor, M. J.; Hamor, T. A.; Hoard, J. L. *J. Am. Chem. Soc.* **1964**, *86*, 1938. (d) Senge, M. O.; Kalisch, W. *Inorg. Chem.* **1997**, *36*, 6103.
- (22) (a) Gouterman, M. In *The Porphyrins*; Dolphin, D., Ed.; Academic Press: New York, 1978; Vol. 3, pp 1–165 (b) Holten, D.; Gouterman, M. In *Optical properties and structure of tetrapyrroles*; Blauer, G., Ed.; de Gruyter: Berlin, 1985; p 63. (c) Dzhagarov, B. M.; Chirvonyi, V. S.; Gurinovich, G. P. In *Laser picosecond spectroscopy and photochemistry of biomolecules*; Letokhov, V. S., Ed.; Hilger: Bristol, 1987; p 137.
- (23) Siebrand, W. *J. Chem. Phys.* **1967**, *46*, 440.
- (24) Michl, J.; Bonačić-Koutecký, V. *Electronic Aspects of Organic Photochemistry*; Wiley-Interscience: New York, 1990.
- (25) (a) Zilberg, S.; Haas, Y. *J. Phys. Chem. A* **1999**, *103*, 2364–2374. (b) Bearpark, M. J.; Bernardi, F.; Clifford, S.; Olivucci, M.; Robb, M. A.; Vreven, T. *J. Phys. Chem. A* **1997**, *101*, 3841.
- (26) (a) Fuss, W.; Hofer, T.; Hering, P.; Kompa, K. L.; Lochbrunner, S.; Schikarski, T.; Schmid, W. E. *J. Phys. Chem.* **1996**, *100*, 921–927. (b) Fuss, W.; Hering, P.; Kompa, K. L.; Lochbrunner, S.; Schikarski, T.; Schmid, W. E.; Trushin, S. A. *Ber. Bunsen-Ges. Phys. Chem.* **1997**, *101*, 500. (c) Samuni, U.; Kahana, S.; Haas, Y. *J. Phys. Chem. A* **1998**, *102*, 4758.
- (27) Ben-Nun, M.; Martinez, T. *J. Chem. Phys. Lett.* **1998**, *298*, 57.
- (28) (a) Hruno, C. P.; Tsutsui, M.; Cullen, D. L.; Meyer, E. F.; Morimoto, C. N.; *J. Am. Chem. Soc.* **1978**, *100*, 6068. (b) Hirayama, N.; Takenaka, A.; Sasada, Y.; Watanabe, E.-I.; Ogoshi, H.; Yoshida, Z.-I. *Bull. Chem. Soc. Jpn.* **1981**, *54*, 998.
- (29) Senge, M. O. *J. Porphyrins Phthalocyanines* **1999**, *3*, 216.
- (30) Gentemann, S.; Leung, S. H.; Smith, K. M.; Fajer, J.; Holten, D. *J. Phys. Chem.* **1995**, *99*, 4330–4334.
- (31) Seybold, P.; Gouterman, M. *J. Mol. Spectrosc.* **1969**, *31*, 1.